A new strategy to design SIW-fed arrays

A. Gómez García, J. Rubio, J.L. Masa-Campos, J. Córcoles, Y. Campos-Roca, R. Gómez Alcalá

Abstract—**In this work, a new full-wave strategy, with very low iteration times, is proposed for the optimization and design of antenna arrays fed by substrate integrated waveguides. The device is decomposed into fixed and modifiable (to be optimized) sections, whose generalized scattering matrices are precomputed. The response of the array is calculated by considering firstly only the interactions between the fixed sections, which are then coupled to the modifiable ones in each iteration of an optimization process. To validate the proposed strategy, a transversal 16-slot antenna array, placed on the top plate of a substrate integrated waveguide, has been designed. A speed-up factor of over 2000 times, compared to general purpose commercial software, has been obtained in this optimization process. The final design presents a 1.05 GHz bandwidth under -10 dB in terms of $|S_{11}|$, a maximum realized gain of 17.5 dBi at 17 GHz, and a 99.95% maximum efficiency (without dielectric and conductor losses).**

Index Terms—**Addition theorems, cylindrical modes, spherical modes, optimization process, antenna array, substrate integrated waveguide (SIW).**

I. INTRODUCTION

SUBSTRATE INTEGRATED WAVEGUIDES (SIW), have been a topic of interest due to their capability to combine the high-power handling properties of traditional rectangular waveguides with the fabrication techniques used in printed circuit boards (PCBs).

Recently, we have presented a new methodology to analyze SIW-based antenna arrays [1]. This methodology is based on a domain decomposition method that segments the array into different sections bounded by cylindrical and spherical ports. Then, addition theorems are simultaneously applied to connect cylindrical waves between the sections defined in the parallel plates region and spherical waves between the array elements on the radiation region. In this way, the full-wave response is obtained with the assumption of an infinite ground plane. The error introduced by this last approximation, in practice, has proven to be negligible.

In this work, the methodology proposed in [1] is accelerated for design purposes by using a new strategy. It is based on precomputing the Generalized Scattering Matrices (GSM) of the sections, and on precomputing the interactions between fixed sections, which are those whose position and geometry do not change. Then, in each iteration cycle in the optimization process, only the interactions between modifiable sections and to fixed sections need to be computed. This strategy takes profit from the fact that the number of fixed (non-optimizable) sections, which includes the metallic vias that define the SIW, is much greater than the modifiable sections, given by slots of variable size in width and length.

The proposed strategy has been used to design a progressive wave 16-slot SIW antenna array by means of the unified third version of the nondominated sorting genetic algorithm (U-NSGA-III) [2]. As a result, a novel design where the physical dimensions of the slots do not follow a monotonic tendency to increase the adaptation, and no additional matching elements are needed, has been obtained. The final design, with a size of $9.17\lambda_0$ at 17 GHz, provides a 17.5 dBi gain near broadside, with over a 1.0 GHz bandwidth under 10 dB in terms of |S11|, and a 99.95% maximum efficiency (without dielectric and conductor losses).

The optimization process is carried out in 12 hours, with only three frequencies being considered, thanks to the new strategy that provides a speedup of 10 w.r.t. [1] and of 2259 w.r.t. CST Studio Suite 2020.

II. THEORY

The new proposed methodology follows the diagram shown in Fig. 1, where a zero step is also included. This zero step refers to the determination of the GSMs of the possible geometries involved in the design process that describe the different sections in which the array can be divided. It is also in this step when the assignation of fixed and modifiable sections occurs.

In general terms, three different sections can be defined in a SIW array: feeders, radiating elements and scatterers. A feeder is defined as any section *i* that relates feeding modes with cylindrical modes. A radiating element is defined as any section *i* that relates cylindrical modes to spherical modes. And, lastly, a scatterer is any section *i* that is only able to relate the cylindrical modes present in its cylindrical port, such as the metallized vias.

This work was supported by FEDER program (European Union) and Junta de Extremadura under projects GR18055 and GR21072; by MINECO/AEI/FEDER, European Union, Spain, under project TEC2017-83352-C2-2-P; by the Spanish Ministry of Science, Innovation and Universities under the State Subprogram for Research Infrastructures and Scientific-Technical Equipment via the RF Prototyping and Measurement Lab with reference EQC2019-005583-P; by the Spanish Government under grant PID2020-116968RB-C32 (DEWICOM) funded by MCIN/AEI/ 10.13039/501100011033 (Agencia Estatal de Investigación); and by the Spanish Ministry of Education, Culture and Sport (MECD) via a PhD grant to A. Gómez García (FPU17/00825)

A. Gómez García, J. Rubio., Y. Campos-Roca and R. Gómez Alcalá are with Escuela Politécnica, Universidad de Extremadura, 10003 Cáceres, Spain. (E-mail: alfonsogg@unex.es, jesusrubio@unex.es, rgomezal@unex.es).

J. L. Masa-Campos and J. Córcoles are with Escuela Politécnica Superior, Universidad Autónoma de Madrid, 28049 Madrid, Spain.

(e-mail: joseluis.masa@uam.es).

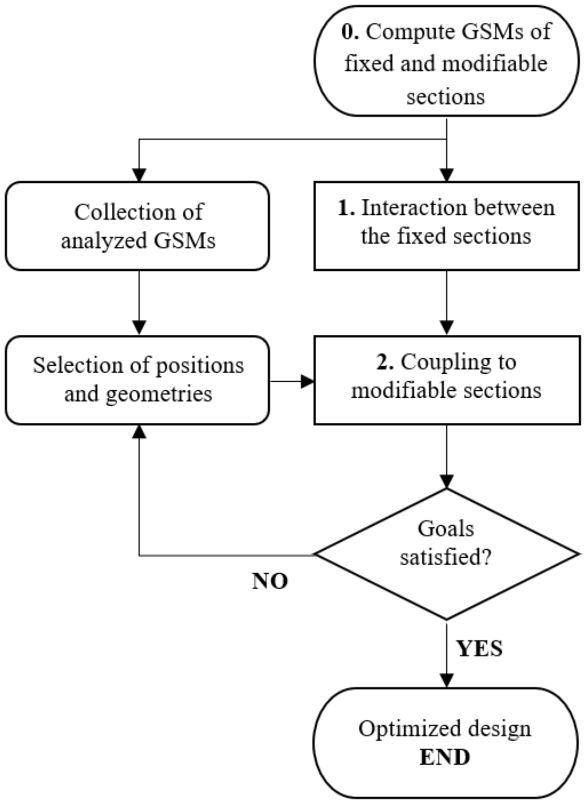

Fig. 1 General block diagram of the new proposed strategy, with optimization loop.

In general, the GSM of one of these sections is given as

$$\begin{bmatrix} \mathbf{\Gamma}^{(i)} & \mathbf{R}_{\mathrm{c}}^{(i)} & \mathbf{R}_{\mathrm{e}}^{(i)} \\ \mathbf{T}_{\mathrm{c}}^{(i)} & \mathbf{S}_{\mathrm{c}}^{(i)} & \mathbf{C}_{\mathrm{ce}}^{(i)} \\ \mathbf{T}_{\mathrm{e}}^{(i)} & \mathbf{C}_{\mathrm{ec}}^{(i)} & \mathbf{S}_{\mathrm{e}}^{(i)} \end{bmatrix} \begin{bmatrix} \mathbf{v}^{(i)} \\ \mathbf{a}_{\mathrm{c}}^{(i)} \\ \mathbf{a}_{\mathrm{e}}^{(i)} \end{bmatrix} = \begin{bmatrix} \mathbf{w}^{(i)} \\ \mathbf{b}_{\mathrm{c}}^{(i)} \\ \mathbf{b}_{\mathrm{e}}^{(i)} \end{bmatrix}, \qquad (1)$$

where $\mathbf{v}^{(i)}$ and $\mathbf{w}^{(i)}$ are column vectors of complex amplitudes of incident and reflected modes, respectively, on the feeding port of section *i*, $\mathbf{a}_{\mathrm{c}}^{(i)}$ and $\mathbf{b}_{\mathrm{c}}^{(i)}$ are column vectors of complex amplitudes of standing and scattered cylindrical modes on the cylindrical port of section *i*, and $\mathbf{a}_{\mathrm{e}}^{(i)}$ and $\mathbf{b}_{\mathrm{e}}^{(i)}$ are column vectors of complex amplitudes of standing and scattered spherical modes on the hemispherical port of section *i*.

There are analytical methods to obtain the GSM of the SIW metallized via holes [3]. For the rest of sections, the finite element/modal analysis solver proposed in [4] is used. The GSM of the different variations of each possible geometry used in the optimization process is also calculated, resulting in a discrete collection of analyzed geometries that can be easily and quickly loaded in each iteration of the optimization process.

In [1], the interactions between the different cylindrical ports are accounted in a single step by means of the general translational matrix for cylindrical modes, $\mathbf{G}_c^{(i,j)}$, which relates the scattered cylindrical modes from the cylindrical port of section *j* to the incident modes of section *i*. An analogous definition is used for the spherical modes, where $\mathbf{G}_e^{(i,j)}$ allows the consideration of arbitrary rotation and translation in a 3D space [5].

However, in this work we adopt a different strategy. Contrary to [1], we first couple the sections that will not change in the optimization process neither in shaper nor position, to later couple the modifiable sections to each other and with the defined fixed sections. As it was proven in [6], in the context of coupling antennas, the result of this strategy is the same as the one obtained if all the sections are coupled simultaneously. This two-step process allows computational time savings if the number of fixed sections is large in comparison to the modifiable ones, since fixed sections are only needed to be coupled once at the beginning (step 1 in Fig. 1).

A. *Interaction between the fixed sections*

In this first step, the interaction between the cylindrical ports of the considered fixed sections are evaluated, since there are no fixed spherical ports. This results in a GSM that establishes a relationship between the fixed-coupled feeding modes and the cylindrical modes scattered by the fixed sections. Submatrices of this GSM are given as

$$\begin{aligned} \mathbf{\Gamma}_{\mathrm{f}}^{(c)} &= \mathbf{\Gamma}_{\mathrm{f}} + \mathbf{R}_{\mathrm{cf}}\mathbf{G}_{\mathrm{cff}}(\mathbf{I} - \mathbf{S}_{\mathrm{cf}}\mathbf{G}_{\mathrm{cff}})^{-1}\mathbf{T}_{\mathrm{cf}} \\ \mathbf{R}_{\mathrm{cf}}^{(c)} &= \mathbf{R}_{\mathrm{cf}} + \mathbf{R}_{\mathrm{cf}}\mathbf{G}_{\mathrm{cff}}(\mathbf{I} - \mathbf{S}_{\mathrm{cf}}\mathbf{G}_{\mathrm{cff}})^{-1}\mathbf{S}_{\mathrm{cf}} \\ \mathbf{T}_{\mathrm{cf}}^{(c)} &= (\mathbf{I} - \mathbf{S}_{\mathrm{cf}}\mathbf{G}_{\mathrm{cff}})^{-1}\mathbf{T}_{\mathrm{cf}} \\ \mathbf{S}_{\mathrm{cf}}^{(c)} &= (\mathbf{I} - \mathbf{S}_{\mathrm{cf}}\mathbf{G}_{\mathrm{cff}})^{-1}\mathbf{S}_{\mathrm{cf}} \end{aligned} \qquad (2)$$

where $\mathbf{\Gamma}_{\mathrm{f}}$, $\mathbf{R}_{\mathrm{cf}}$, $\mathbf{T}_{\mathrm{cf}}$ and $\mathbf{S}_{\mathrm{cf}}$ are block-matrices, whose blocks are the submatrices of the fixed sections: $\mathbf{\Gamma}^{(i)}$, $\mathbf{R}_{\mathrm{c}}^{(i)}$, $\mathbf{T}_{\mathrm{c}}^{(i)}$ and $\mathbf{T}_{\mathrm{c}}^{(i)}$. $\mathbf{G}_{\mathrm{cff}}$ is built from $\mathbf{G}_c^{(i,j)}$by considering only the fixed sections. Other parameters, such as the maximum dimensions of the antenna or the SIW width are also fixed. Henceforth, feeding elements and many via holes can be regarded as fixed.

B. *Coupling to modifiable sections*

The second step of the proposed strategy is also the iterated step in an optimization process. In this step, the previously determined GSMs are used in conjunction with an iterated set of defined positions and geometries of the modifiable sections.

The procedure followed to couple the modifiable sections formally is identical to the one followed in [1]. Therefore, we can use the expressions obtained there to calculate the scattering parameters between the feeding ports of the SIW, as well as for the transmission matrix that relates amplitudes of feeding ports with amplitudes of spherical modes radiated by each element. Once interactions between all elements have been calculated

$$[\mathbf{\Gamma} + \mathbf{R}_{\mathrm{c}}\mathbf{G}_{\mathrm{c}}\mathbf{P}\mathbf{T}_{\mathrm{c}} + (\mathbf{R}_{\mathrm{e}}\mathbf{G}_{\mathrm{e}} + \mathbf{R}_{\mathrm{c}}\mathbf{G}_{\mathrm{c}}\mathbf{P}\mathbf{C}_{\mathrm{ce}}\mathbf{G}_{\mathrm{e}})\mathbf{M}^{-1}\mathbf{Q}]\mathbf{v} = \mathbf{w} \qquad (3)$$

$$\mathbf{M}^{-1}\mathbf{Q}\mathbf{v} = \mathbf{b}_{\mathrm{e}}, \qquad (4)$$

with

$$\mathbf{P} = (\mathbf{I} - \mathbf{S}_\mathrm{c}\mathbf{G}_\mathrm{c})^{-1}$$

$$\mathbf{M} = \mathbf{I} - \mathbf{S}_\mathrm{e}\mathbf{G}_\mathrm{e} - \mathbf{C}_\mathrm{ec}\mathbf{G}_\mathrm{c}\mathbf{P}\mathbf{C}_\mathrm{ce}\mathbf{G}_\mathrm{e}$$

$$\mathbf{Q} = \mathbf{T}_\mathrm{e} + \mathbf{C}_\mathrm{ec}\mathbf{G}_\mathrm{c}\mathbf{P}\mathbf{T}_\mathrm{c}\ .$$

However, in this case it should be observed that the interactions between cylindrical ports of fixed sections have already been carried out, so that they must be removed from (3) and (4). For this purpose

$$\mathbf{G}_\mathrm{c} = \begin{pmatrix} \mathbf{G}_\mathrm{cmm} & \mathbf{G}_\mathrm{cmf} \\ \mathbf{G}_\mathrm{cfm} & \mathbf{0} \end{pmatrix}. \tag{5}$$

In addition, fixed sections with spherical ports do not contain cylindrical ports

$$\mathbf{C}_\mathrm{ce} = \begin{pmatrix} \mathbf{C}_\mathrm{cem} \\ \mathbf{0} \end{pmatrix};\ \mathbf{C}_\mathrm{ec} = \begin{pmatrix} \mathbf{C}_\mathrm{ecm} & \mathbf{0} \end{pmatrix}$$

and they do not contain feeding ports either

$$\mathbf{R}_\mathrm{e} = (\mathbf{0});\ \ \mathbf{T}_\mathrm{e} = (\mathbf{0})$$

since feeding ports are fixed and they only connect to cylindrical ports

$$\mathbf{T}_\mathrm{c} = \begin{pmatrix} \mathbf{0} \\ \mathbf{T}_\mathrm{cf}^{(c)} \end{pmatrix};\ \ \mathbf{R}_\mathrm{c} = \begin{pmatrix} \mathbf{0} & \mathbf{R}_\mathrm{cf}^{(c)} \end{pmatrix};\ \mathbf{\Gamma} = \begin{pmatrix} \mathbf{\Gamma}_\mathrm{f}^{(c)} \end{pmatrix}$$

On the other hand, scattering from cylinders must be considered for fixed and for modifiable sections but, in the first case, it should be noted that fixed cylinders have previously been coupled between them

$$\mathbf{S}_\mathrm{c} = \begin{pmatrix} \mathbf{S}_\mathrm{cm} & \mathbf{0} \\ \mathbf{0} & \mathbf{S}_\mathrm{cf}^{(c)} \end{pmatrix}.$$

The greatest effort to compute (3) and (4) is focused on obtaining $\mathbf{P}$. However, instead of calculating $\mathbf{P}$ through direct inversion, we use the block-wise matrix inversion technique. The fact that such matrix, to be inverted, can be broken down into sub-blocks is advantageous, hence

$$\mathbf{I} - \mathbf{S}_\mathrm{c}\mathbf{G}_\mathrm{c} = \begin{pmatrix} \mathbf{I} - \mathbf{S}_\mathrm{cm}\mathbf{G}_\mathrm{cmm} & -\mathbf{S}_\mathrm{cm}\mathbf{G}_\mathrm{cmf} \\ -\mathbf{S}_\mathrm{cf}^{(c)}\mathbf{G}_\mathrm{cfm} & \mathbf{I} \end{pmatrix}.$$

After applying block-wise inversion, (3) reduces to

$$\left[\mathbf{\Gamma}_\mathrm{f}^{(c)} + \mathbf{R}_\mathrm{cf}^{(c)}\mathbf{G}_\mathrm{cfm}\mathbf{V}(\mathbf{S}_\mathrm{cm} + \mathbf{C}_\mathrm{cem}\mathbf{G}_\mathrm{e}\mathbf{M}^{-1}\mathbf{Q})\right]\mathbf{v} = \mathbf{w}, \tag{6}$$

with

$$\mathbf{M} = \mathbf{I} - (\mathbf{S}_\mathrm{e} + \mathbf{B}\mathbf{C}_\mathrm{cem})\mathbf{G}_\mathrm{e}$$

$$\mathbf{Q} = (\mathbf{B}\mathbf{S}_\mathrm{cm} + \mathbf{C}_\mathrm{ecm})\mathbf{G}_\mathrm{cmf}\mathbf{T}_\mathrm{cf}^{(c)}$$

$$\mathbf{B} = \mathbf{C}_\mathrm{ecm}(\mathbf{G}_\mathrm{cmm} + \mathbf{A})\mathbf{V}$$

$$\mathbf{A} = \mathbf{G}_\mathrm{cmf}\mathbf{S}_\mathrm{cf}^{(c)}\mathbf{G}_\mathrm{cfm}$$

$$\mathbf{V} = \left(\mathbf{I} - \mathbf{S}_\mathrm{cm}(\mathbf{G}_\mathrm{cmm} + \mathbf{G}_\mathrm{cmf}\mathbf{S}_\mathrm{cf}^{(c)}\mathbf{G}_\mathrm{cfm})\right)^{-1}.$$

Since the number of fixed sections is much greater than the modifiable sections, the main computational effort of this step is multiplying three matrices of dimensions $nm\times nf$, $nf\times nf$, and $nf\times nm$, where nf is the total number of cylindrical modes used in the fixed sections and nm is its counterpart for modifiable sections. The previous work in [1] required the inversion of a matrix with dimensions $(nm+nf)\times(nm+nf)$, thus obtaining faster iteration times in an optimization process.

This step results in the complete full-wave analysis of the device, obtaining both the final S-parameters of the feeding modes and the radiation pattern of the array.

III. Optimization Process And Obtained Results

In this section, we will cover the design of a progressive-wave 16 transversal slot SIW-fed 1D linear array antenna. The device is based on a Rogers RT/Duroid 5880 substrate, and is designed to operate at 17 GHz, suitable for satellite communications or radar positioning applications.

The optimization methodology is briefly summarized, and the computational time using the proposed methodology, the previous work exposed in [1], and CST Studio Suite 2020 [7] is compared. After that, the obtained final design is also validated with CST Studio Suite 2020.

A. Optimization Process

The U-NSGA-III genetic algorithm [2] provided with pymoo [8], considering Riesz s-Energy directions [9], is used to design the array. The optimized parameters are the length and width of each individual slot, and the distance between consecutive slots, adding to a total of 47 individual variables to optimize. The fixed sections are made of 2 feeders and 162 pairs of metallized vias, resulting in 2310 fixed modes. The modifiable sections account for the 16 antennas, totaling in 384 spherical modes and 240 cylindrical modes.

The length of the slots is discretized into 32 values, ranging from 4.0 mm to 8.0 mm. The width is discretized into 7 values, from 0.3 mm to 1.2 mm. The distance between consecutive slots varies between 7.83 mm and 16.53 mm.

Four different optimization goals are established. In terms of $|S_{11}|$, the goal is to obtain less than −20 dB at 17 GHz, and −15 dB at 16.85 GHz and 17.15 GHz. For $|S_{21}|$, the goal is a magnitude lower than -30 dB at 17 GHz. The gain is to be maximized between θ = -10º y θ = 10º in the array (φ = 0º) plane at 17 GHz. The last goal is to minimize the side lobe level, in the same plane at the same frequency.

A total of 48 generations with 2350 individuals are calculated in the optimization process, resulting in 112800 iterations. Table 1 shows a comparison of the CPU execution time per calculated frequency point between CST Studio Suite 2020, [1] and this work. The first part of the comparison is the GSM computation of the feeder, and of each possible one of 224 slots configurations. The analysis time is defined as the needed to obtain the complete response of the device from the start of the optimization process. And iteration time refers to the time needed to obtain the complete response of the design when some part of it is modified. This key difference implies that only the coupling to the modifiable sections needs to be redone in such cases.

The obtained speedup factor implies that, if single frequency optimization goals are defined, the complete optimization process detailed, with full-wave accuracy in each iteration, takes only 4 hours to finish with the new proposed strategy. By contrast, the same optimization process takes 38 hours with [1], and renders the general purpose CST Studio Suite 2020 only useful for the subsequent validation step.

B. *Obtained Results*

Fig. 2 shows the simulated lossless results, obtained with the full-wave methodology and CST Studio Suite 2020. An excellent agreement can be observed between the two, both in terms of S-parameters and radiation gain, with all the proposed optimization goals being fulfilled. A 1.05 GHz bandwidth under -10 dB in $|S_{11}|$ is obtained, while the simulated $|S_{21}|$ at 17 GHz is -50 dB. The realized gain is 17.5 dBi at 17 GHz, while the total efficiency of the simulated design is 99.95% at 17 GHz, equal to the impedance mismatch factor for this lossless simulation.

IV. Conclusion

In this work, we have presented a new strategy to design SIW-fed arrays. Its usefulness has been validated by performing a design of a 16-slot SIW-fed array. The proposed strategy is several times faster than a previous work and allows for an optimization process unaffordable with general purpose software, being completely carried out in 12 hours.

References

[1] J. Rubio, A. G. Garcia, R. G. Alcala, J. Garcia, and Y. Campos-Roca, "Simultaneous Use of Addition Theorems for Cylindrical and Spherical Waves for the Fast Full-Wave Analysis of SIW-Based Antenna Arrays," *IEEE Trans. Antennas Propag.*, vol. 67, no. 12, pp. 7379–7386, 2019, doi: 10.1109/TAP.2019.2930175.

[2] H. Seada and K. Deb, "A Unified Evolutionary Optimization Procedure for Single, Multiple, and Many Objectives," *IEEE Trans. Evol. Comput.*, vol. 20, no. 3, pp. 358–359, 2016, doi: 10.1109/TEVC.2015.2459718.

[3] E. Díaz Caballero, H. Esteban, Á. Belenguer, and V. Boria, "Efficient analysis of substrate integrated waveguide devices using hybrid mode matching between cylindrical and guided modes," *IEEE Trans. Microw. Theory Tech.*, vol. 60, no. 2, pp. 232–243, 2012, doi: 10.1109/TMTT.2011.2178424.

[4] J. Rubio, M. A. González, and J. Zapata, "Analysis of cavity-backed microstrip antennas by a 3-D finite element/segmentation method and a matrix lanczos-padé algorithm (SFELP)," *IEEE Antennas Wirel. Propag. Lett.*, vol. 1, pp. 193–195, 2002, doi: 10.1109/LAWP.2002.807783.

[5] J. E. Hansen, *Spherical near-field antenna measurements*, vol. 26. London, UK: Peter Peregrinus Ltd., 1988.

[6] J. F. Izquierdo, J. Rubio, and J. Zapata, "Antenna-generalized scattering matrix in terms of equivalent infinitesimal dipoles: Application to finite array problems," *IEEE Trans. Antennas Propag.*, vol. 60, no. 10, pp. 4601–4609, 2012, doi: 10.1109/TAP.2012.2207348.

[7] C. S. Technology and Dassault Systèmes Vélizy-Villacoublay France, "Cst Studio Suite ™ 2020." 2020, [Online]. Available: https://www.3ds.com/es/productos-y-servicios/simulia/productos/cst-studio-suite/.

[8] J. Blank and K. Deb, "Pymoo: Multi-Objective Optimization in Python," *IEEE Access*, vol. 8, pp. 89497–89509, 2020, doi: 10.1109/ACCESS.2020.2990567.

[9] J. Blank, K. Deb, Y. Dhebar, S. Bandaru, and H. Seada, "Generating Well-Spaced Points on a Unit Simplex for Evolutionary Many-Objective Optimization," *IEEE Trans. Evol. Comput.*, vol. 25, no. 1, pp. 48–60, 2021, doi: 10.1109/TEVC.2020.2992387.

Table 1
CPU Simulation Time Per Calculated Frequency Point On A Xeon E-2167G (3.70 GHz) For The Performed Optimization Process

	CST	**Using** [1]	**This work**
GSM computation (Step 0)	N.A.	805.1s	805.1s
Analysis time (Steps 1+2)	282.36s	1.21s	1.53s
Iteration time (Step 2)	282.36s	1.21s	0.12s
Iteration Speedup factor (w.r.t. to CST)	x1	x233	x2259

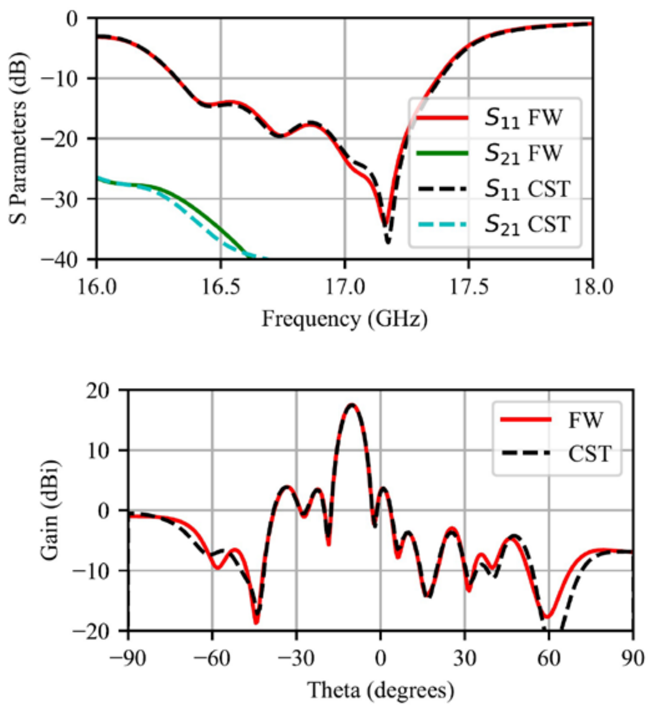

Fig. 2 Simulated s-parameters (top) and realized gain at 17 GHz in the φ = 0º plane (bottom) of the lossless optimized design. FW refers to the results obtained with the proposed methodology.